Coupling of blocking and melting in cobalt ferrofluids

Tianlong Wen,[1,a)] Wenkel Liang,[2] and Kannan M. Krishnan[1,b)]
[1]*Department of Materials Science and Engineering, University of Washington, Box 352120, Seattle, Washington 98195-2120, USA*
[2]*Department of Chemistry, University of Washington, Box 351700, Seattle, Washington 98195-1700, USA*

(Presented 19 January 2010; received 29 October 2009; accepted 21 December 2009; published online 19 April 2010)

Zero-field-cooling and field-cooling (FC) measurements were performed on ferrofluids of cobalt magnetic nanoparticles (MNPs) in various organic solvent. Two peaks, one broad peak corresponding to the blocking transition (T_B), and one sharp peak corresponding to the melting of the solvent (T_M), were observed. Furthermore, for a given MNP size, when the blocking and melting transitions were superposed by choosing an appropriate solvent, the strongest intensity of the sharp peak at the melting point of the organic solvent was obtained. This observation is explained by applying the M spectrum theory. Additionally, a first order, melting-induced magnetic phase transformation was observed at the melting point of the solvent. Associated with the first order phase transition and the supercooling effect, a thermal hysteresis loop in the FC curve was observed.
 [doi:10.1063/1.3350901]

Ferrofluids (FFs) containing magnetic nanoparticles (MNPs) with single domains and superparamagnetic at room temperature[1] and well-dispersed in a carrier fluid are both of fundamental[2] and applied interest in biomedicine,[3] mechanical[4] and sensor technologies,[5] and room temperature magnetic refrigerators.[6] Although FFs have been investigated for some time,[7] there are still many ambiguities about their fundamental properties including aging and memory effects,[8] related slow dynamics,[8] and phase transitions.[9] Typically, in zero-field-cooling (ZFC) and field-cooling (FC) experiments of FFs, two phase transitions are observed;[10] i.e., a characteristic peak (T_B) corresponding to the blocking transition of the superparamagnetic system[11] and additionally, a sharp peak (T_M) during the melting of the solvent in the ZFC curve. Here we focus on the peak at T_M and show that its intensity is dependent on the relative position of T_B and T_M. We observe the strongest peak at T_M when the two phase-transition temperatures coincide, i.e., $T_B \sim T_M$, but its intensity is dramatically reduced when they are well separated. We explain this observation by the reactivated and strongest Brownian relaxation of cobalt MNPs when $T_B \sim T_M$ by inspecting the M spectrum[8] of the FFs.

Cobalt MNPs were fabricated by the well-established thermal decomposition procedure[12] by rapid injection of cobalt carbonyl $[Co_2(CO)_8]$ into a solution of 1,2-dichlorobenzene at 182 °C in the presence of surfactants under an inert Argon atmosphere to prevent cobalt nanoparticles from oxidization. The as-synthesized cobalt MNPs, passivated by a layer of surfactant (~2 nm) to prevent aggregation and oxidation, were then washed, precipitated by ethanol, and dried in a glass vial. The mass of the cobalt nanoparticles was estimated by taking the mass difference of the vial after the cobalt MNPs were completely dried. Then 4 mg dried cobalt MNPs were dissolved in 0.2 ml organic solvents, and were sonicated for 1 h to make uniform and stable cobalt FFs. After that, these cobalt FFs were sealed in a gelatin capsule, and their magnetic properties were measured in a Quantum Design Physical Property Measurement System. For the ZFC measurement, the cobalt FFs were cooled from room temperature with no external magnetic field to 10 K, then a magnetic field, H=100 Oe, was applied at 10 K, and then the magnetization of the sample was measured as a function of increasing temperature. For the FC measurement, the magnetization of the sample was measured both during cooling (FCC) and warming (FCW) under an external magnetic field of 100 Oe.

During the ZFC and FC measurements, there are two mechanisms that involves the relaxation of the magnetization directions of individual cobalt MNPs, namely, the Néel relaxation (rotation of only the magnetization direction with the Co MNPs being physically fixed in position) and Brownian relaxation (physical rotation of cobalt MNPs with magnetization direction fixed along an easy axis).[13] The Néel relaxation time is $\tau_N = \tau_o \exp(\Delta E/k_B T)$, where $\tau_0 \sim 10^{-9}-10^{-11}$ s and when a field H is applied, $\Delta E = KV(1-h)^2$, where K is the anisotropy constant, V is the volume of cobalt MNPs, $h = H/H_K$ is the reduced field, and H_K is the effective anisotropy field.[13] In the weak field measurement, $H \ll H_K$, $h \sim 0$; as a result, $\tau_N = \tau_o \exp(KV/k_B T)$. The Brownian relaxation time is $\tau_B = 3V_H \eta/k_B T$, where V_H is the hydrodynamic volume of the cobalt MNPs including the coating, and η is the dynamic viscosity of the carrier liquid.[13] Due to the exponential increase in the Néel relaxation time and a linear increase in the Brownian relaxation time with size of cobalt MNPs, smaller particles prefer Néel relaxation, while larger particles prefer Brownian relaxation. The completely frozen FFs behave like magnetic nanocomposites,[14] where the MNPs are embedded in a solid matrix. However, as the temperature increases above a critical point below the melting point of the organic solvent, the frozen organic solvent begins to melt starting from the interface between the matrix and the nanoparticles as expected for an incoherent interface.[15] As a result, there are three distinct relaxation

a)Electronic mail: halong@u.washington.edu.
b)Electronic mail: kannanmk@u.washington.edu.

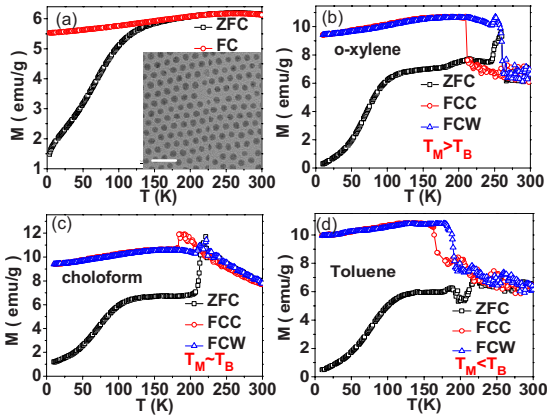

FIG. 1. (Color online) ZFC and FC curves for cobalt MNP (a) powders, and in o-xylene (b), chloroform (c), and toluene (d). H=100 Oe for all measurements. FCC and FCW are the field cooling curves during decreasing and increasing temperatures, respectively. The scale bar of the inset in (a) is 40 nm.

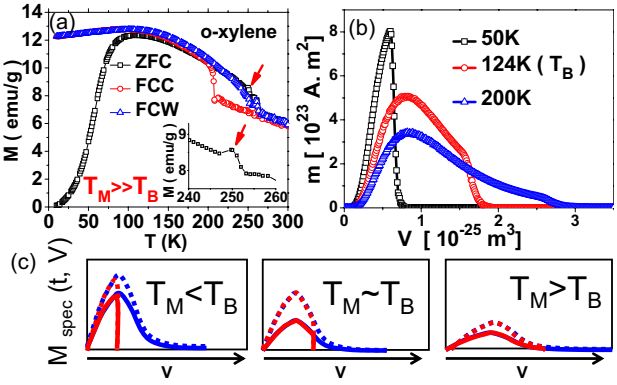

FIG. 2. (Color online) ZFC/FC curve (H=100 Oe) for well separated melting and blocking temperatures (a), very small peak (marked by arrow) observed during melting, and the inset shows the magnified peak of the ZFC curve in the vicinity of T_M of o-xylene; (b) the simulated ZFC M spectrum of 5 nm cobalt MNPs with a log normal size distribution and a standard deviation of 1 nm approximated at 50 K, 124 K (T_B) and 200 K, respectively (Ref. 8), for 10^{18} particles; and (c) the schematic M spectrum of ZFC and FC (solid lines) and the corresponding enhanced M spectrum of ZFC and FC (dashed lines) by adding the effect of Brownian relaxation that aligns easy axis of Co MNPs to the external magnetic field.

stages/phases as the temperature is increased from 10 K to room temperature, namely: (I) completely frozen stage below a critical premelting temperature T_{PM}, where the system behaves like a magnetic nanocomposite, and only Néel relaxation is permitted; (II) premelting stage at temperature $T_{PM} < T < T_M$, with the presence of an interfacial liquid between cobalt MNPs and the frozen organic solvent. At this stage, cobalt MNPs are spatially fixed as in the completely frozen stage, however, the Brownian relaxation of Cobalt MNPs is restored due to the presence of a surrounding liquid; and (III) completely melting stage above T_M, where cobalt MNPs can diffuse by both rotation and translation, and both Néel relaxation and Brownian relaxation are present.

Figures 1(a)–1(d) show the ZFC/FC curve of cobalt MNPs powders, cobalt MNP FFs in o-xylene (T_M=248 K), chloroform (T_M=210 K) and toluene (T_M=180 K), respectively. The downturn in FC magnetization of both powders and FFs as temperature decreases, at low temperature, is sensitive to the strong dipole-dipole interactions between cobalt nanoparticles,[8] strongly influencing the Néel relaxations of the cobalt MNPs (Ref. 9) and thereby affecting T_B. Hence, T_B is chosen for the specific FF and not for the cobalt MNPs as in Ref. 10. The reading of the blocking temperature of the cobalt MNP powders in Fig. 1(a) is ~250 K from the maximum magnetization of ZFC measurement, which is consistent with the TEM observation of 9 nm cobalt[16] shown as an inset in Fig. 1(a). The temperature corresponding to the blocking transition is shifted to ~210 K after these particles are dispersed and diluted in the organic solvent due to larger particle separation and thus lower interparticle interactions[17] in FFs, as indicated by the peak at $T_B \sim 210$ K in Fig. 1(b). The organic solvents and concentration of cobalt MNPs are chosen such that $T_M > T_B$ in o-xylene in Fig. 1(b), $T_M \sim T_B$ in chloroform in Fig. 1(c), and $T_M < T_B$ in toluene in Fig. 1(d). In the ZFC measurement, another sharp peak, in addition to one at $T_B \sim 210$ K, was observed during the melting of o-xylene (T_M=248 K) in Fig. 1(b). The dramatic increase in the ZFC magnetization in Fig. 1(b) starts from T ~243 K, which is below the melting temperature of o-xylene. This sharp peak occurs at the stage II of premelting as mentioned above. After that, the ZFC magnetization drops rapidly with increasing temperature, which corresponds to the stage III or complete melting. When the cobalt MNPs were dispersed in chloroform ($T_M \sim T_B$), the two peaks corresponding to the blocking transition of the Co MNPs and the melting of chloroform are superposed on each other to yield a sharp peak of much greater intensity, followed by a quick drop after complete melting as in o-xylene. Finally, when the cobalt MNPs were dispersed in the toluene ($T_M < T_B$), the two peaks of blocking and melting are separated again; however, the peak due to melting is observed at a lower temperature followed by a quick drop of ZFC magnetization due to the complete melting of toluene. After that, a broad peak due to the blocking transition is observed at temperature ~210 K in the liquid phase. It is worth mentioning that the dramatic increase in the ZFC magnetization during melting starts before the melting temperature of the solvent in both chloroform and toluene as in o-xylene. The strongest peak at T_M is observed when the transition of blocking and melting is coupled together, but is expected to be greatly reduced when they are separated as explained below by the M spectrum theory.[8] To verify the latter, FF containing cobalt MNPs of smaller size in o-xylene was prepared so that the blocking (~100 K) and the melting (248 K) are well separated. As expected and shown in Fig. 2(a), a sharp peak but of greatly reduced intensity was observed during melting of o-xylene. The enhancement of the FC magnetization of the FFs, compared with the cobalt MNPs in powder form, as shown in Fig. 1, is due to the additional possibility of Brownian relaxation of cobalt MNPs in FFs under external magnetic field during cooling.

The M spectrum,[8] defined by the integrand in $\overline{M}(t) = \int M_{spec}(t, V) dV$ for particles of volume V at time t, used to explain aging and memory effects in interacting and noninteracting systems, can also be applied to the observed FC and ZFC behavior of these FFs. It can be calculated[8] by the product of the particle volume distribution functions, f(V), and

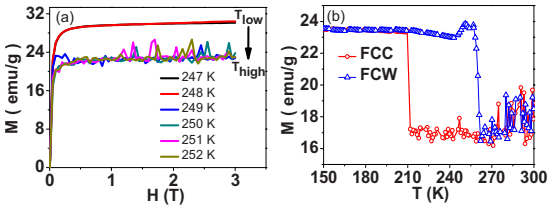

FIG. 3. (Color online) (a) The jump of the M(H,T) curve during the melting of the solvent, indicates a first order melting induced magnetic phase transformation. The measurement is performed from low temperature to high temperature. (b) Thermal hysteresis loop of Co MNPs in o-xylene with an external magnetic field of 500 Oe.

the magnetization of a single particle of volume, V, at time t, $M(t,V)$, namely, $M_{spec}(t,V)=M(t,V)\ f(V)$. At a specific temperature, the M spectra of ZFC and FC magnetization are superposed on each other for particles with volume less than a critical value, V_B, because all smaller Co MNPs are always unblocked and will reach the same equilibrium magnetic state under the same external magnetic field in ZFC and FC measurement. However, for particles with volume larger than the critical volume, V_B, the M spectrum of the ZFC measurement [the red lines in Fig. 2(c)] will drop to zero due to the randomly blocked nature of the larger particles; however the M spectrum for FC measurement [the blue lines in Fig. 2(c)] is still nonzero due to the predetermined magnetic configuration during cooling under an external magnetic field.[8] As temperature increases, V_B, defining the cutoff of ZFC in the M spectrum, moves to higher values because the larger nanoparticles begin to be unblocked while the intensity of the M spectrum is reduced due to thermal agitation [see the simulation for Co MNPs in Fig. 2(b)]. During the premelting stage (II) of the carrier fluid, the Brownian relaxation, quenched previously, is reactivated to allow the cobalt MNPs to also rapidly rotate their easy axes physically, under the influence of the external magnetic field. This enhances the value of the M spectrum [dashed line in Fig. 2(c)], leading to a sudden increase in the ZFC magnetization as indicated by the observed sharp peak during melting. The area enclosed by the two ZFC lines (red) in the M spectra, proportional to the intensity of the peak during melting, is largest when T_B and T_M coincide, as shown in Fig. 2(c). As a result, the largest intensity of the sharp peak during melting is observed when the blocking and melting are coupled together. Furthermore, as mentioned above, the smaller cobalt MNPs do not favor Brownian relaxation, resulting in a smaller intensity increase in the M spectrum for the smaller cobalt MNPs. Consequently, the area enclosed by the M spectra for these two ZFC curves is small for the case of $T_M < T_B$ [Fig. 2(c)] and a sharp peak with greatly reduced intensity of the ZFC magnetization at 180 K is observed [Fig. 1(d)].

Figure 3(a) shows the isothermal M(H,T) curves of cobalt FF in the vicinity of the melting point of o-xylene. The M(H) curves change continuously with respect to the temperature below the bulk melting point of o-xylene; while a jump in the isothermal M(H) curve has been observed at the melting point. The sudden jump of the isothermal M(H) curve at the melting point of the organic solvent indicates the occurrence of a first order magnetic phase transformation, and is accompanied by the sudden drop of the FCW magnetization in Fig. 3(b). As mentioned above, the transformation from the premelting stage (II) to the complete melting stage (III) will occur at the melting point of the solvent. As a result, this first order magnetic phase transformation is a melting induced magnetic phase transformation, where the state of cobalt MNPs with spatially fixed locations (stage II) is transformed to a state when the position of the cobalt MNPs evolves randomly (stage III) even though both Néel relaxation and Brownian relaxation are present in the two distinct states. Furthermore, as the liquid is cooled through its melting point from high temperature, the solidification will not occur until the temperature is well below the melting point. This supercooling phenomenon[18] results in the first order magnetic phase transformation to occur at ~210 K in the FCC magnetization, as shown in Fig. 3(b). The first order phase transformation and the associated supercooling effects, lead to the observed thermal hysteresis loop [Fig. 3(b)] in the FC curve during cooling and heating.

In conclusion, a sharp peak (T_M) on the ZFC curve of cobalt FFs during melting, activated by the Brownian relaxation, can be mostly enhanced by coinciding with the blocking transition (T_B) of the Co MNPs. In addition, a thermal hysteresis is observed due to a first order magnetic phase-transition at the melting point and the supercooling effect of the organic solvent. Coupling of the tunable first order (T_M) and second order (T_B) magnetic phase transformations in such FFs might be of interest to the magnetocaloric effect[19] and such work is also in progress.

This project is partially supported by National Science Foundation DMR Contract No. 0501421 and the Murdock Foundation. Part of this work was conducted at the UW-NTUF, a member of NSF-NNIN.

[1] K. M. Krishnan, A. B. Pakhomov, Y. Bao, P. Blomqvist, Y. Chun, M. Gonzales, K. Griffin, X. Ji, and B. K. Roberts, J. Mater. Sci. **41**, 793 (2006).
[2] B. Huke and M. Lücke, Rep. Prog. Phys. **67**, 1731 (2004).
[3] Q. A. Pankhurst, J. Connolly, S. K. Jones, and J. Dobson, J. Phys. D **36**, R167 (2003).
[4] K. Raj, B. Moskowitz, and R. Casciari, J. Magn. Magn. Mater. **149**, 174 (1995).
[5] S. H. Chung, A. Hoffmann, S. D. Bader, C. Liu, B. Kay, L. Makowski, and L. Chen, Appl. Phys. Lett. **85**, 2971 (2004).
[6] R. E. Rosensweig, Int. J. Refrig. **29**, 1250 (2006).
[7] S. Odenbach, J. Phys.: Condens. Matter **16**, R1135 (2004).
[8] M. Sasaki, P. E. Jönsson, H. Takayama, and H. Mamiya, Phys. Rev. B **71**, 104405 (2005).
[9] J. Zhang, C. Boyd, and W. Luo, Phys. Rev. Lett. **77**, 390 (1996).
[10] M. B. Morales, M. H. Phan, S. Pal, N. A. Frey, and H. Srikanth, J. Appl. Phys. **105**, 07B511 (2009).
[11] M. F. Hansen and S. Mørup, J. Magn. Magn. Mater. **203**, 214 (1999).
[12] V. F. Puntes, K. M. Krishnan, and A. P. Alivisatos, Science **291**, 2115 (2001).
[13] R. Kötitz, P. C. Fannin, and L. Trahms, J. Magn. Magn. Mater. **149**, 42 (1995).
[14] X. Batlle and A. Labarta, J. Phys. D **35**, R15 (2002).
[15] R. W. Cahn, Nature (London) **323**, 668 (1986).
[16] Y. Bao and K. M. Krishnan, J. Magn. Magn. Mater. **293**, 15 (2005).
[17] J. García-Otero, M. Porto, J. Rivas, and A. Bunde, Phys. Rev. Lett. **84**, 167 (2000).
[18] F. C. Frank, Proc. R. Soc. London, Ser. A **215**, 43 (1952).
[19] V. K. Pecharsky and K. A. Gschneidner, Jr., Appl. Phys. Lett. **70**, 3299 (1997).